Journal of Macromolecular Science, Part A
Publication details, including instructions for authors and subscription information:
http://www.informaworld.com/smpp/title~content=t713597274

Chitooligosaccharide Copolymers: Synthesis and Aqueous Self-assembly

Sanping Zhao[a]; Min-Kyung Lee[a]; Jonghwi Lee[a]
[a] Department of Chemical Engineering and Materials Science, Chung-Ang University, Seoul, S. Korea

Online publication date: 26 April 2010

To cite this Article Zhao, Sanping , Lee, Min-Kyung and Lee, Jonghwi(2010) 'Chitooligosaccharide Copolymers: Synthesis and Aqueous Self-assembly', Journal of Macromolecular Science, Part A, 47: 6, 580 — 587
To link to this Article: DOI: 10.1080/10601321003741982
URL: http://dx.doi.org/10.1080/10601321003741982

Journal of Macromolecular Science, Part A: Pure and Applied Chemistry (2010) **47**, 580–587

ISSN: 1060-1325 print / 1520-5738 online
DOI: 10.1080/10601321003741982

Taylor & Francis
Taylor & Francis Group

Chitooligosaccharide Copolymers: Synthesis and Aqueous Self-assembly

SANPING ZHAO**, MIN-KYUNG LEE and JONGHWI LEE*

Department of Chemical Engineering and Materials Science, Chung-Ang University, Dongjak-gu, Seoul, S. Korea

Received January 2009, Accepted February 2010

Novel water-soluble amphiphilic graft copolymers (COS-g-PCL-b-MPEG) were synthesized by the coupling reaction between chitooligosaccharide (COS) and MPEG-b-PCL-COOH, which was synthesized via ring-opening polymerization of ε-caprolactone (CL) using MPEG as an initiator and subsequent carboxylation by succinic anhydride. The chemical composition of the graft copolymers was confirmed by ^{1}H-NMR spectra and FT-IR spectrometry. The thermal properties and crystallinity of the copolymers were observed by DSC and XRD measurements, which showed the existence of separate backbone and graft chain phases in the copolymer. The micellar behavior via self-assembly of the graft copolymers in aqueous solution was studied using pyrene fluorescence dye technique. AFM measurements showed that the micelles had a spherical morphology at the critical micelle concentration (CMC) and ranged in size from 20–45 nm. The amphiphilic ternary biodegradable graft copolymer endows the hydrophilic outer shell of micelles with structural and functional diversification, which might be desirable for drug delivery applications.

Keywords: Chitooligosaccharide, graft copolymer, micelle, self-assembly, water-soluble polymer

1 Introduction

Amphiphilic copolymers can self-assemble into micelles with core-shell structures in a selective solvent. The micelles have thermodynamically stable nano-structures which can be spherical, cylindrical or wormlike, depending on the type of solvent and the block ratios of polymer (1–3). These copolymers have been extensively studied in the biotechnology and pharmaceutical fields to improve the therapeutic efficiency of drugs or other agents that can be incorporated into the inner core of polymeric micelles (4–7).

Recently, polymeric micelles with poly(ethylene glycol) (PEG) as the hydrophilic, shell-forming block have attracted interest in pharmaceutical applications due to their prolonged blood circulation time (8, 9). As the hydrophobic, core-forming blocks, polyesters such as poly(lactic acid) (PLA), poly(glycolic acid) (PGA), poly(lactic acid-*co*-glycolic acid) (PLGA), and poly(ε-caprolactone) (PCL) have attracted special attention because of their biodegradability and biocompatibility, as well as high drug-loading capacity due to their hydrophobic properties, all of which makes them attractive for drug delivery systems (10). These poly(ether-ester) diblock or triblock copolymers (AB, ABA, or BAB type) have successfully been studied as carriers for many hydrophobic drugs (11–14).

For these amphiphilic block copolymers with long polyester segments, the most common protocols for preparing aqueous solutions of micelles or drug-loaded micelles involve the dissolution of the copolymer and drug in a mixture of an organic solvent for the hydrophobic block and water, followed by solvent evaporation or dialysis of the solution against water (15, 16). However, it is difficult to completely remove organic solvents, which limits the potential of these micelles for biomedical applications. Moreover, it was demonstrated that a method using organic cosolvent with water affected the self-assembly of the block copolymer (17). A few researchers have developed solvent-free methods to incorporate drugs into self-assembled polymeric micelles by simply dissolving amphiphilic copolymers in water (18). The production of solvent-free drug-loaded micelles is more favorable for *in vivo* applications. An additional limitation of applications that use micelles derived from poly(ether-ester) amphiphilic block copolymers is the difficult structural modification of the PEG-based shell (19). To address this issue, Shuai et al. (20) prepared hyperbranched PEI-g-PCL-b-PEG for gene vectors by combining the high transfection efficiency of branched polyethylenimine (PEI) and the amphiphilic structure of PCL-b-PEG block copolymers.

*Address correspondence to Jonghwi Lee, Department of Chemical Engineering and Materials Science, Chung-Ang University, 221 Heukseok-dong, Dongjak-gu, Seoul 156-756, S. Korea. Tel: 82-02-820-5269; FAX: 82-02-824-3495; E-mail: jong@cau.co.kr
**E-mail: zhaosanping@163.com

The present study was concerned with the synthesis of novel water-soluble ternary COS derivates via conjugation of amphiphilic MPEG-b-PCL diblock copolymer onto chitooligosaccharide backbone. Chitooligosaccharide (COS), the oligomer of chitosan, is obtained by the chemical or enzymatic hydrolysis of chitosan, which is soluble in a neutral aqueous solution. COS exhibits favorable biological activities such as anti-microbial and anti-tumor activities and DNA complexation capability. Moreover, COS contains hydroxyl and amino groups for further chemical modification. These unique properties make COS attractive for use in biomaterial applications (21, 22). MPEG-b-PCL grafts endow COS with amphiphilicity, which is important for efficient drug loading. The amphiphilic graft copolymers are expected to self-assemble into micelles with hydrophobic PCL as the core-forming blocks and hydrophilic COS and PEG as the double shell-forming blocks in aqueous solution. This cationic functional COS copolymer consisting of PEG and readily biodegradable PCL might be more suitable for *in vivo* drug delivery applications. In this study, we investigated the synthesis, micellar behavior of amphiphilic ternary COS derivatives, and morphology of the micelles.

2 Experimental

2.1 Materials

Chitooligosaccharide (COS) with a 95% deacetylation and number-average molecular weight of 10 Kg/mol (KITTO LIFE, Korea) was dried at 60°C for 2 days under vacuum before use. ε-Caprolactone (99%, Aldrich, USA) was dried over CaH2 for 2 days and distilled under vacuum just before use. Mono-methoxy(polyethylene glycol) (MPEG, Aldrich, USA) of Mn =2000 g/mol was used after drying under vacuum at 100°C for 24 h. Stannous 2-ethyl hexanoate (95%, Sigma, USA) was used as received.

4-Dimethylaminopyridine (DMAP, 99%), succinic anhydride (SA, 98%), and trimethylamine (TEA, 99%) (TCI, Japan) were used as received. Dicyclohexylcarbodiimide (DCC, 99%) and N-hydroxysuccinimide (NHS, 99%) were purchased from Aldrich (USA). Tetrahydrofuran (THF) and dimethyl sulfoxide (DMSO) (HPLC grade) were distilled over CaH2 before use. The other chemicals were analytical grade and were used without further purification.

2.2 Synthesis of MPEG-b-PCL-COOH

MPEG-b-PCL-OH was first synthesized via ring-opening polymerization of ε-caprolactone monomer using hydroxyl-terminated MPEG as an initiator and stannous 2-ethyl hexanoate ($Sn(Oct)_2$) as a catalyst. Briefly, MPEG (10 g, 5 mmol), ε-caprolactone (3.42 g, 30 mmol), and $Sn(Oct)_2$ (13 mg) were introduced into a 100 mL single-necked round-bottom flask equipped with a magnetic stirring bar in dry nitrogen atmosphere, which was degassed by a vacuum pump for 20 min and purged with nitrogen gas. The degassing and purging process was repeated three times. The ring-opening polymerization was carried out at 125°C in a nitrogen atmosphere for 16 h. The product was purified by precipitating into anhydrous diethyl ether from chloroform solution and dried under vacuum at 40°C. The yield was around 90 wt%.

Carboxyl-terminated MPEG-b-PCL monomer was prepared with succinic anhydride in the presence of DMAP and trimethylamine (TEA) following the method described in the literature (23, 24). MPEG-b-PCL (10 g), succinic anhydride (0.46 g), DMAP (0.47 g), and TEA (0.5 mL) were dissolved in dried THF (120 mL) and left at room temperature for 24 h. The product was precipitated using anhydrous diethyl ether. The unreacted succinic anhydride was removed by filtration after dissolving the mixture in chilled methylene chloride. The product was purified by precipitating into anhydrous diethyl ether from methylene chloride solution twice, and then dried at 40°C under reduced pressure for 2 days.

2.3 Synthesis of COS-g-PCL-b-MPEG Copolymers

COS-g-PCL-b-MPEG graft copolymers with different compositions were synthesized by coupling reactions between chitooligosaccharide and carboxyl-terminated MPEG-b-PCL using DCC as a coupling agent, as shown in Scheme 1. Dried COS and carboxyl-terminated diblock copolymers with different molar ratios were dissolved in dried DMSO (0.5 g COS with 60 mL DMSO), followed by the addition of DCC and NHS as coupling agents (4 and 2 mole equivalent to the carboxyl-terminated MPEG-b-PCL copolymer, respectively) in a nitrogen atmosphere. The reaction was maintained at room temperature for 48 h under continuous stirring. The mixture was precipitated by adding an excess of anhydrous diethyl ether. After the precipitant was dissolved in DMSO, the solution was dialyzed with a cellulose membrane (molecular weight cut-off: 12,000-14,000 g/mol) against DMSO for 3 days and distilled water for another 3 days to remove the unreacted MPEG-b-PCL-COOH and other impurities, and the sample was then freeze-dried to obtain graft copolymer powders.

2.4 ^{1}H-NMR and FT-IR Measurements

^{1}H-NMR spectra were recorded on a Varian UI500 NMR spectrometer at 500 MHz at room temperature with CDCl3 as the solvent for MPEG-b-PCL and MPEG-b-PCL-COOH, and D2O for the graft copolymers. FT-IR spectra were recorded using KBr discs on a Magna 750 FT-IR spectrometer (Nicolet, USA) at room temperature.

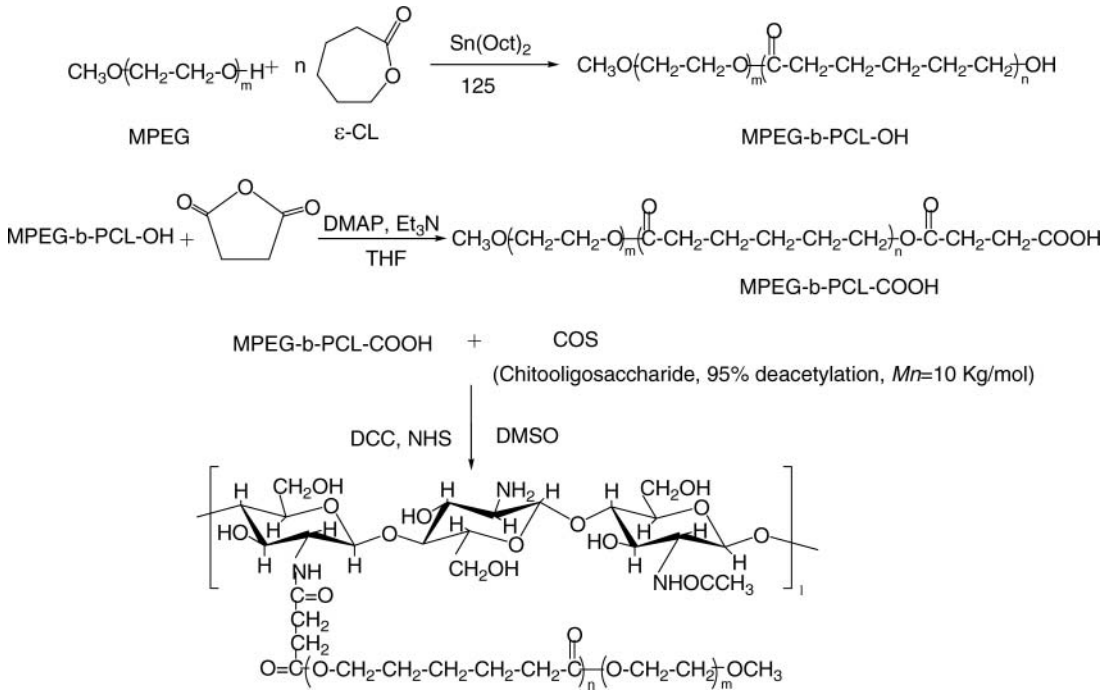

Sch. 1. Schematic illustration for synthesis of COS-g-PCL-b-MPEG graft copolymer.

2.5 Thermal Analysis

A differential scanning calorimeter (DSC) (DSC-Q100, TA Instrument, UK) was used to measure the thermal properties of the polymers. The DSC thermograms covered a temperature range of –20 to 80°C at a scanning rate of 5°C/min.

2.6 XRD Analysis

X-ray diffraction (XRD) measurements were performed on a Rigaku D/Max-2500/PC type X-ray diffractometer. The radiation source was nickel-filtered Cu-Kα radiation with a wavelength of 0.154 nm, and the voltage and current were set to 40 kV and 40 mA, respectively. The proportional counter detector collected data at a rate of $2\theta = 1°$/min over the range $2\theta = 5$–$35°$.

2.7 Steady-State Fluorescence Measurements

Steady-state fluorescence spectra were recorded on an AB2 luminescence spectrometer (Aminco-Bowman, France). Pyrene was used as a hydrophobic fluorescent probe (25, 26). A solution of pyrene in THF was added to distilled water, and the THF was removed by stirring at 40°C for 4 h. The final concentration of pyrene was 1×10^{-6} M. Graft copolymer concentrations ranging from 5×10^{-4} to 1 mg/mL were prepared by dissolving and diluting the solution. The solutions were kept at room temperature for 24 h to reach the solubilization equilibrium of pyrene in the aqueous phase. Excitation spectra were monitored at 334 nm at 25°C and emission spectra ranging from 350 to 440 nm were recorded. Both excitation and emission bandwidths were 8 nm.

2.8 Atomic Force Microscopy Measurements

Atomic force microscopy (AFM) images were recorded with a XE-100 (PSIA, Korea). The samples for AFM measurement were prepared as follows. A COS-g-MPCL$_{14}$ solution was prepared by directly dissolving the graft copolymer in distilled water (the concentration of graft copolymer: 0.04 mg/mL, near the critical micelle concentration (CMC)). The solution was dropped on a freshly cleaved mica surface, and the mica was rapidly frozen in liquid nitrogen. Then, the frozen micellar solution on the mica wafer was lyophilized for 24 h to remove water.

3 Results and Discussion

3.1 Synthesis and Characterization of Graft Copolymers

Water-soluble graft copolymers with different MPEG-b-PCL contents were synthesized via coupling reaction between COS and carboxyl-terminated amphiphilic MPEG-b-PCL copolymer (Scheme 1). To obtain the carboxyl-terminated MPEG-b-PCL copolymer, the MPEG-b-PCL diblock copolymer was first synthesized via the ring-opening polymerization of ε-*c*aprolactone using MPEG as an initiator and stannous 2-ethyl hexanoate ($Sn(Oct)_2$) as a catalyst. The product was then reacted with succinic

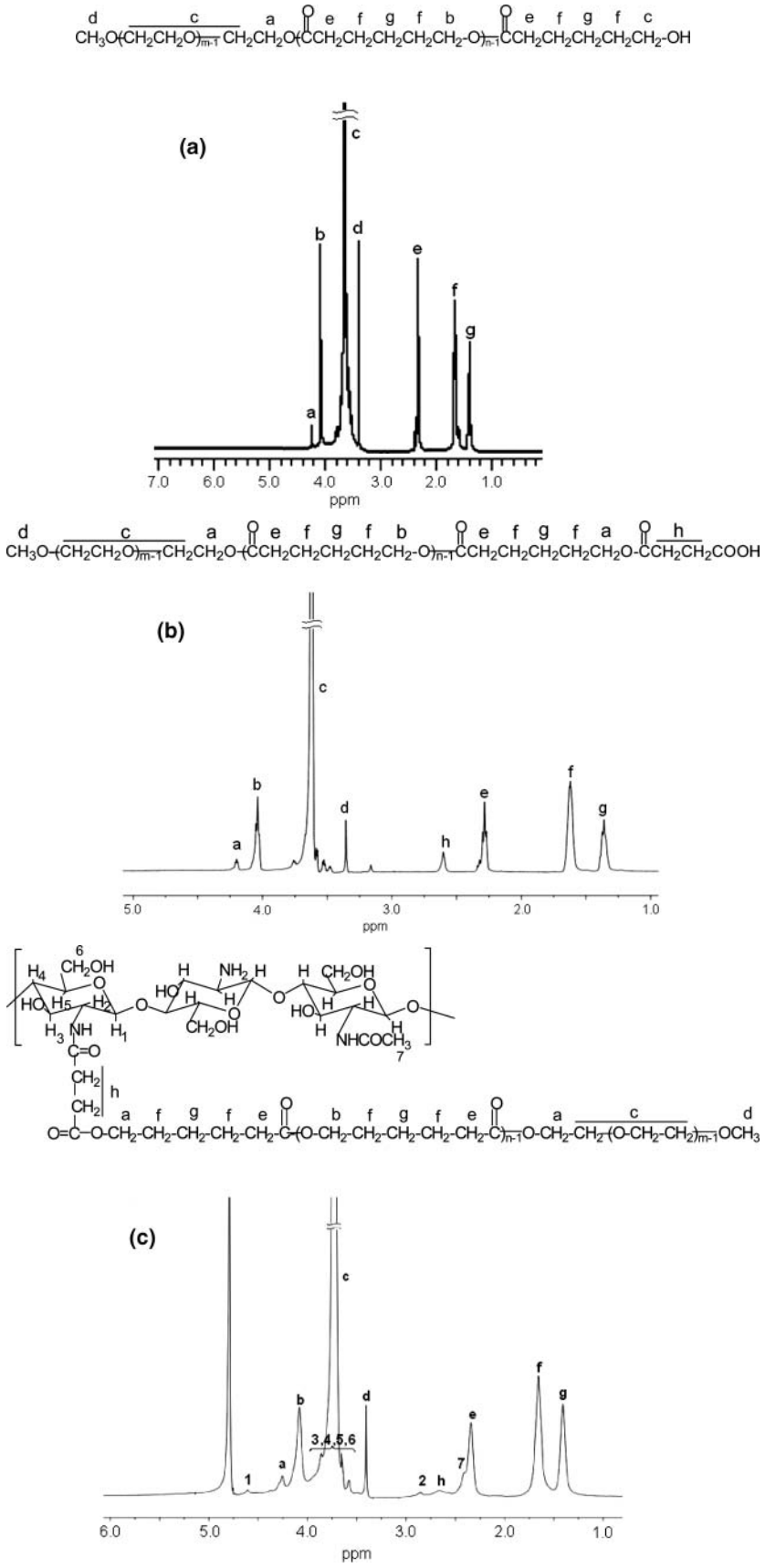

Fig. 1. ^{1}H-NMR spectra of $MPEG_{45}$-b-PCL_6 diblock copolymer (a), carboxyl-terminated $MPEG_{45}$-b-PCL_6 (b), and COS-g-$MPCL_{14}$ (c).

anhydride using DMAP and TEA as catalysts. To make the carboxyl-terminated diblock copolymer water-soluble, the feed molar ratio of CL to MPEG was kept at 6. Figure 1a and b exhibit the ^{1}H-NMR spectra of the $MPEG_{45}$-b-PCL_6 diblock copolymer and $MPEG_{45}$-b-PCL_6-COOH. The small peak at 4.22 ppm belongs to methylene protons of the PCL-CO-OCH_2-CH_2-O-MPEG segment (Figure 1a), indicating the successful synthesis of diblock copolymer. The composition of the diblock copolymer, calculated from the peak intensities of the -CH_2CH_2- protons in the MPEG block (~3.63 ppm) and the -CH_2- protons in the PCL block (~4.04 ppm), was found to be 5.7, which nearly coincided with the feed molar ratio of CL to MPEG (27). Moreover, the conjugation of the succinic anhydride (SA) to the obtained $MPEG_{45}$-b-PCL_6-OH was verified by ^{1}H-NMR as shown in Figure 1b. The singlet peak at 2.61 ppm is characteristic of the protons of an SA moiety after ring opening (28). The ratio of the integration of this peak to that of the peak for CH_3O- in the MPEG block (Figure 1b) suggested that ca. 90% of the diblock copolymer chains had been functionalized.

The graft copolymer was prepared by conjugation of carboxyl-capped $MPEG_{45}$-b-PCL_6 copolymer onto the COS backbone under DCC and NHS in DMSO. Figure 1c is the ^{1}H-NMR spectrum of the graft copolymer, which shows the proton signals of COS at 3.0-5.0 ppm (29), the methylene proton signals of carboxyl-terminated $MPEG_{45}$-b-PCL_6 diblock copolymer are also clearly confirmed. The average number of $MPEG_{45}$-b-PCL_6 grafts per COS was calculated from the ratio of the integrated areas of the methyl signal (CH_3-O-) of MPEG segment at 3.4 ppm and H1 signal of COS at 4.6 ppm. The chemical compositions could be varied by changing the feed molar ratio of carboxyl-terminated $MPEG_{45}$-b-PCL_6 to COS (Table 1).

The FT-IR spectra of COS, carboxyl-capped $MPEG_{45}$-b-PCL_6 and the graft copolymers are shown in Figure 2. The FT-IR spectrum of COS showed two characteristic peaks (30) for amide I band and amide II band around 1657 and 1560 cm^{-1}, respectively. In the spectra of graft copolymers we observed the characteristic peaks from COS and $MPEG_{45}$-b-PCL_6 branches, including the ester carbonyl stretching band (C=O, around 1740cm^{-1}), the C-O stretching band (around 1110 cm^{-1}) of the PEG segment, and C-H stretching band (3000–2850 cm^{-1}) of PEG and PCL segments. Moreover, the relative intensities of the peaks

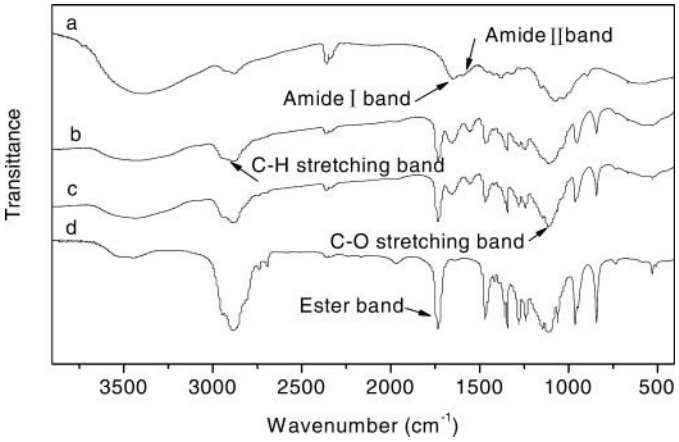

Fig. 2. FT-IR spectra of COS (a), COS-g-$MPCL_{14}$ (b), COS-g-$MPCL_{31}$ (c), and carboxyl-capped $MPEG_{45}$-b-PCL_6 (d).

from the C=O group (mainly from PCL segment), the C-O group in the PEG segment and the C-H stretching of PCL and PEG segments increased as the number of $MPEG_{45}$-b-PCL_6 grafts increased. All of our results suggested that we had achieved a successful synthesis of the graft copolymers.

3.2 Thermal Properties and Crystallinity of Graft Copolymers

Figure 3 shows the second melting curves of COS, graft copolymers, and $MPEG_{45}$-b-PCL_6-COOH. COS did not show any melting transition over the experimental temperature range. Therefore, the thermal behaviors detected by DSC measurements could be attributed to $MPEG_{45}$-b-PCL_6 side chains in the graft copolymers. The value of the melting temperature (T_m) (Table 1) of $MPEG_{45}$-b-PCL_6–COOH shifted to a lower temperature after it was grafted onto the COS backbone. This may be due to the fact that the existence of COS in the graft copolymer hinders the formation of more regular crystalline domains. For graft copolymers, the value of ΔH increases and T_m shifts to higher temperatures as the number of $MPEG_{45}$-b-PCL_6 grafts increases.

Figure 4 shows the X-ray diffraction patterns of COS, graft copolymers and $MPEG_{45}$-b-PCL_6-COOH. The broader weak peak of COS at around $2\theta = 19^\circ$ indicates

Table 1. Synthesis and characteristic of COS-g-MPEG-b-PCL graft copolymers

Designations	*COS mmol*	*$MPEG_{45}$-b-PCL_6-COOH mmol*	*No. of grafts*[a]	*yield (%)*	*CMC*[b] *mg/mL*	*T_m °C*	*ΔH J/g*
COS-g-$MPCL_{14}$	0.05	1	14	67.3	0.040	44.1	69.3
COS-g-$MPCL_{31}$	0.05	2	31	72.2	0.030	46.4	82.2
$MPEG_{45}$-b-PCL_6-COOH	–	–	–	85.5	0.0034	50.4	136.4

[a]Calculated from ^{1}H-NMR.
[b]Determined using the pyrene fluorescence dye technique (25, 26).

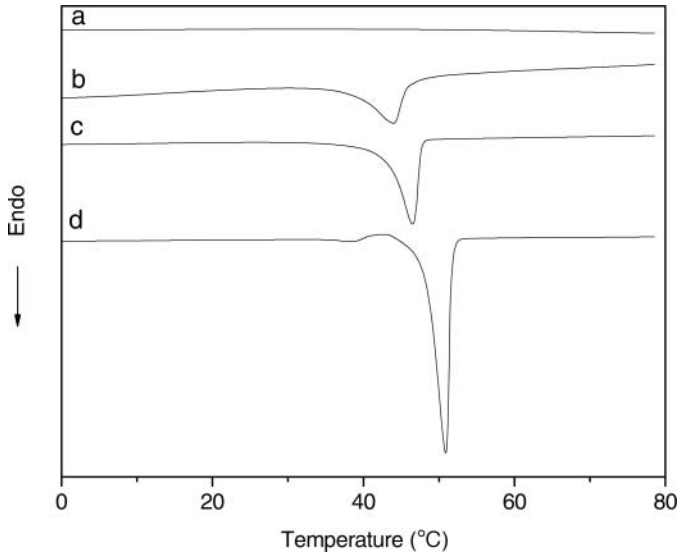

Fig. 3. Second heating DSC curves for COS (a), COS-g-$MPCL_{14}$ (b), COS-g-$MPCL_{31}$ (c), and carboxyl-capped $MPEG_{45}$-b-PCL_6 (d).

that COS has an amorphous structure, very different from its precursor, chitosan, which has strong reflections at $2\theta = 10$ and 20°.[31] For the two graft copolymer samples, two strong characteristic peaks appeared at $2\theta = 19.1°$ and $2\theta = 23.3°$, which could be attributed to the crystal phase of the $MPEG_{45}$-b-PCL_6 grafts. In comparison with the $MPEG_{45}$-b-PCL_6-COOH diblock copolymer, the graft copolymers had broader and weaker peaks, suggesting that COS hindered the crystallization of $MPEG_{45}$-b-PCL_6 segments, which is consistent with the DSC results. However, as the number of grafts increased in the graft copolymers, the peak intensity became stronger. These results reveal that

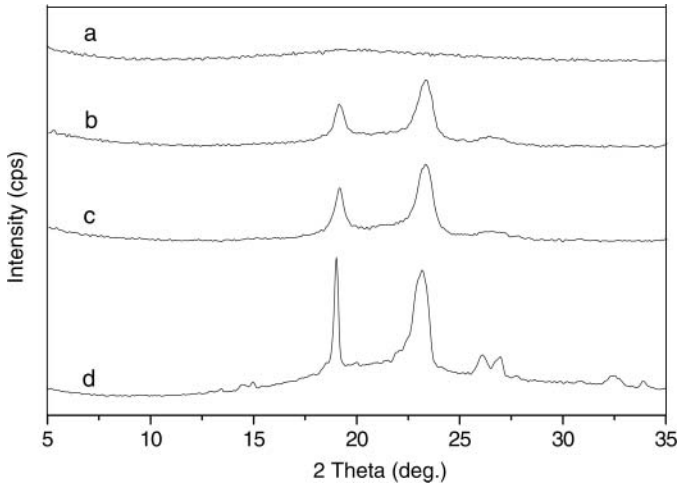

Fig. 4. X-ray diffraction patterns for COS (a), COS-g-$MPCL_{14}$ (b), COS-g-$MPCL_{31}$ (c), and carboxyl-capped $MPEG_{45}$-b-PCL_6 (d).

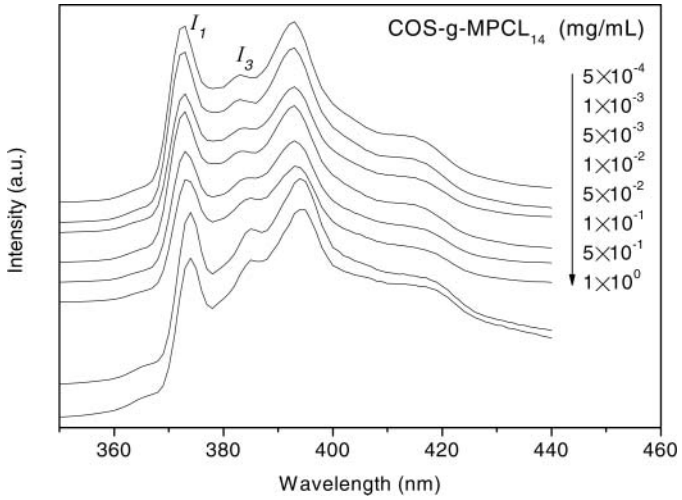

Fig. 5. Emission spectra of pyrene in the COS-g-$MPCL_{14}$ copolymer solution at a fixed excitation wavelength of 334 nm. The concentration of pyrene was 1×10^{-6} M.

the graft copolymers have two separate phases; amorphous COS and semicrystalline graft chain.

3.3 Micellar Behaviors of Graft Copolymers in Aqueous Solution

COS, the oligomer of chitosan, is soluble in neutral aqueous solution, but chitosan is only soluble in acid aqueous solution. Herein, by grafting water-soluble $MPEG_{45}$-b-PCL_6 diblock copolymer with a relatively shorter PCL segment to a COS backbone, the obtained graft copolymers can dissolve in neutral aqueous media at room temperature. Since the structure of ternary graft copolymers is composed of hydrophobic and hydrophilic moieties, polymeric micelles are expected to form by the direct dissolution of graft copolymers in distilled water.

In this study, the fluorescence probe, pyrene, was used to evaluate the critical micelle concentration (CMC) values of obtained graft copolymers. Figure 5 shows the emission spectra of pyrene in the presence of graft copolymer. The pyrene quantum yield increases due to the decreased polarity of the environment, and the CMC can be determined using the characteristic peak shifts (25, 26). Because the intensity of the I_1 peak gradually decreases with the incorporation of pyrene into the hydrophobic core region of the micelles from water, the intensity ratio of I_3/I_1 indicates the change in micelle concentration.

Figure 6 shows the intensity ratio of I_3/I_1 of the pyrene excitation spectra as a function of the logarithm of graft copolymer concentration. Below the CMC, the intensity ratio was low and the slope was negligible. When the concentration reached the CMC, the intensity ratio sharply increased. As shown in Figure 6, the intersection of the two tangent curves, a horizontal curve at low graft copolymer concentrations and the inflection, was determined to be

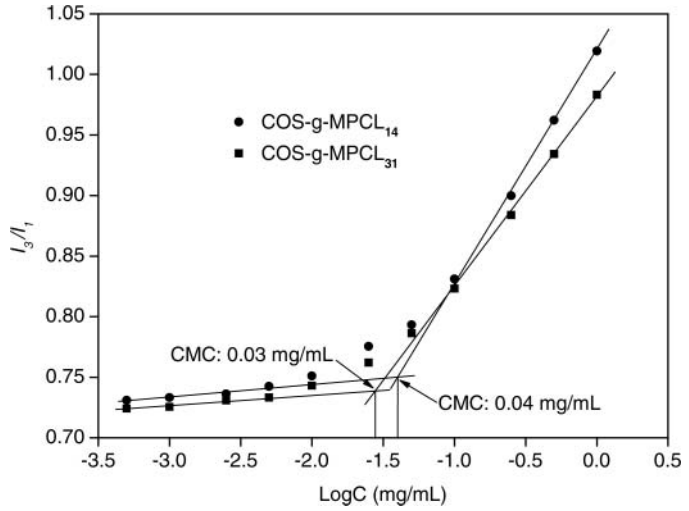

Fig. 6. Intensity ratio I_3/I_1 in the emission spectra as a function of copolymer concentration, C.

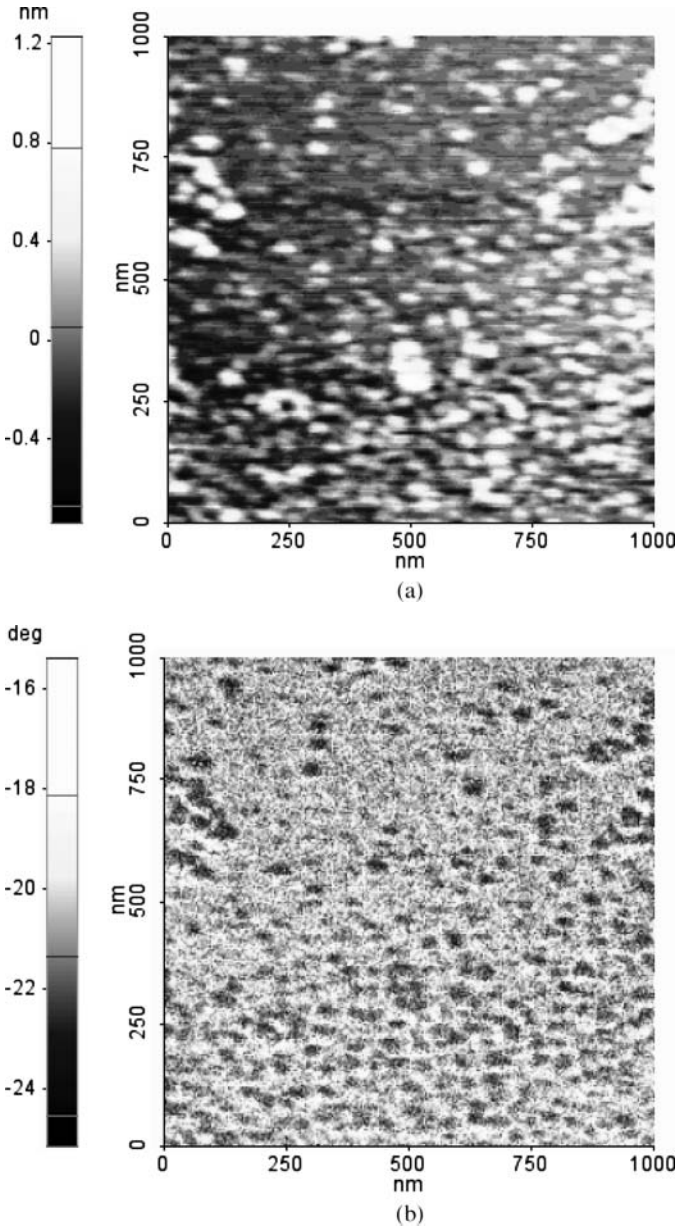

Fig. 7. AFM images of micelles from COS-g-MPCL$_{14}$ aqueous solution at 0.04 mg/mL (near CMC): (a) height and (b) phase image.

the CMC. The CMC values for COS-g-PECL14 and COS-g-PECL31 were 4.0×10^{-2} and 3.0×10^{-2} mg/mL, respectively, both of which are lower than that of the MPEG$_{45}$-b-PCL$_6$ diblock copolymer (3.4×10^{-3} mg/mL) (32). This difference can be attributed to the direct covalent connection that produces a strong interaction between the two blocks. The values are quite low in comparison with those of linear amphiphilic block copolymers (33, 34). This is attributed to the architecture of the graft copolymers. The high graft degree of the copolymer and strong hydrophobic character of the PCL segments led to a very strong tendency towards formation of micelles in aqueous solution, despite a relatively short PCL segment. The CMC values of the graft copolymers slightly decreased as the graft degree in the copolymer increased because of the presence of more hydrophobic PCL segments.

3.4 Morphologies of the Micelles at the CMC

To investigate the morphology of micelles at the CMC, freeze-dried samples were prepared for AFM measurement. The freeze-drying method was adopted to retain the most natural micelle morphology possible in aqueous solution (35). The micelles were formed by directly dissolving the graft copolymer into distilled water to avoid the effects of organic solvents on the morphology of the polymeric micelle (17).

Figure 7 shows the height (a) and phase images (b) of COS-g-MPCL$_{14}$ micelles at a concentration of 0.04 mg/mL (near the CMC). The micelles are separately dispersed on the surface of the mica with an almost spherical morphology. The nano-sized micelles observed on the surface were not uniform, averaging 20–45 nm in diameter. When the concentration of the graft copolymer solution is near the CMC, the hydrophobic segments of the graft copolymer begin to aggregate, resulting in micelle formation. At this stage, we found that a large amount of solvent was trapped in the loose micellar cores and coronas (36).

4 Conclusions

Water-soluble ternary graft copolymers composed of COS as a hydrophilic backbone and amphiphilic MPEG$_{45}$-b-PCL$_6$ diblock copolymers as grafts were successfully synthesized via conjugation between COS and carboxyl-terminated MPEG$_{45}$-b-PCL$_6$ under DCC and NHS. In solid state, the copolymers had separate phases of COS

and graft chains, and in aqueous solution, spherical micelles of 20–45 nm formed at the CMC. The CMC values measured by the steady-state pyrene fluorescence technique decreased as the graft degree of the copolymers increased. These biodegradable ternary graft copolymers can potentially be used as nanocarriers for delivery of hydrophobic drugs or other agents.

Acknowledgments

This work was supported by a grant from the Fundamental R&D Program for Core Technology of Materials funded by the Ministry of Commerce, Industry and Energy, Republic of Korea. SZ would like to thank Human Resource Development BK21 (Korea Research Foundation).

References

1. Zhang, L. and Eisenberg, A. (1996) *J. Am. Chem. Soc.*, 118, 3168-3181.
2. Liu, X., Kim, J.S., Wu, J. and Eisenberg, A. (2005) *Macromolecules*, 38, 6749–6751.
3. Chen, Z., Cui, H., Hales, K., Li, Z., Qi, K., Pochan, D.J. and Wooley, K.L. (2005) *J. Am. Chem. Soc.*, 127, 8592–8593.
4. Kabanov A.V. and Alakhov, V.Y. *Amphiphilic Block Copolymers: Self-Assembly and Applications* (P. Alexamdris, and B. Lindman, Eds.) Elsevier, Netherlands, 1997.
5. Inoue, T., Chen, G., Nakamae, K. and Hoffman, A.S. (1998) *J. Controlled Release.*, 51, 221–229.
6. Teng, Y., Morrison, M.E., Munk, P., Webber, S.E. and Prochazka, K. (1998) *Macromolecules*, 3, 3578–3587.
7. Soga, O., Nostrum, C.F., Fens, M., Rijcken, C.J.F., Schiffelers, R.M., Storm, G. and Hennink, W.E. (2005) *J. Controlled Release*, 103, 341–353.
8. Claesson, P. (1993) *Colloids and Surfaces A: Physicochemical and Engineering Aspects.*, 77, 109–118.
9. Kataoka, K., Harada, A. and Nagasaki, Y. (2001) *Adv. Drug Delivery Rev.*, 47, 113–131.
10. Jeong, B., Kim, S.W. and Bae, Y.H. (2002) *Adv. Drug Delivery Rev.*, 54, 37–51.
11. Davies, M.C., Illum, L., Davis, S.S., Harding, S.E., Purkiss, S. and Gellert, P.R. (1996) *Langmuir*, 12, 2153–2161.
12. Allen, C., Yu, Y., Maysinger, D. and Eisenberg, A. (1998) *Bioconjugate Chemistry.*, 9, 564–572.
13. Allen, C., Han, J., Yu, Y., Maysinger, D. and Eisenberg, A. (2000) *J. Controlled Release.*, 63, 275–286.
14. Shin, I.L.G., Kim, S.Y., Lee, Y.M., Cho, C.S. and Sung, Y.K. (1998) *J. Controlled Release.*, 51, 1–11.
15. La, S.B., Okano, T. and Kataoka, K. (1996) *J. Pharm. Sci.*, 85, 85–90.
16. Zhang, X., Jackson, J.K. and Burt, H.M. (1996) *Int. J. Pharm.*, 132, 195–206.
17. Vangeyte, P., Gautier, S. and Jerome, R. (2004) *Colloids Surfaces A, Physicochemical and Engineering Aspects.*, 242, 203–211.
18. Lin, W.J., Flanagan, D.R. and Linhardt, R.J. (1999) *Polymer*, 40, 1731–1735.
19. Yokoyama, M., Kwon, G.S., Okano, T., Sakurai, Y., Seto, T. and Kataoka, K. (1992) *Bioconjugate Chemistry*, 3, 295–301.
20. Shuai, X., Merdan, T., Unger, F., Wittmar, M. and Kissel, T. (2003) *Macromolecules*, 36, 5751–5759.
21. Roehrig, H., Schmidt, J., Walden, R., Czaja, I., Miklasevics, E. and Wieneke, U. (1995) *Science*, 269, 841–843.
22. Ohara, N., Hayashi, Y., Yamada, S., Kim, S.K., Matsunaga, T. and Yanagiguchi, K. (2004) *Biomaterials*, 25, 1749–1754.
23. Jeon, O., Lee, S.H., Kim, S.H., Lee, Y.M. and Kim, Y.H. (2003) *Macromolecules*, 36, 5585–5592.
24. Wang C.H. and Hsiue, G.H. (2005) *Bioconjugate Chemistry*, 16, 391–396.
25. Kalyanasundaram K. and Thomas, J.K. (1977) *J. Am. Chem. Soc.*, 99, 2039–2044.
26. Wilhelm, M., Zhao, C., Wang, Y. and Xu, R. (1991) *Macromolecules*, 24, 1033–1040.
27. Zhao, S.P., Zhang, L.M. and Ma, D. (2006) *J. Phys. Chem. B*, 110, 12225–12229.
28. Du,Y.J. and Brash, J.L. (2003) *J. Appl. Polym. Sci.*, 90, 594–607.
29. Wang, C.Q., Li, G.T., Tao, S.Y., Guo, R.R. and Yan, Z. (2006) *Carbohydrate Polymers*, 64, 466–472.
30. Sugimoto, M., Morimoto, M., Sashiwa, H., Saimoto, H. and Shigemasa, Y. (1998) *Carbohydrate Polymers*, 36, 49–59.
31. Huh, K.M., Cho, Y.W. and Yui, N. (2004) *Macromol. Biosci.*, 4, 92–99.
32. Zhao, S.P., Lee, J.H. (2008) *Macromol. Res.*, in press.
33. Jeong, B., Bae, Y.H. and Kim, S.W. (1999) *Colloid and Surfaces B: Biointerfaces*, 16, 185–193.
34. Li, J., Li, X., Ni, X. and Wang, X. (2006) *Biomaterials*, 27, 4132–4140.
35. Zhang, Y.Q., Guo, S.R., Lu, C.F. and Liu, L. (2007) *J. Polym. Sci.: Part A: Polym. Chem.*, 45, 605–613.
36. Gao Z.S. and Eisenberg, A. (1993) *Macromolecules*, 26, 7353–7360.